Research Journal of Applied Sciences, Engineering and Technology 7(24): 5163-5171, 2014
DOI:10.19026/rjaset.7.913
ISSN: 2040-7459; e-ISSN: 2040-7467

Submitted: February 08, 2014 Accepted: March 08, 2014 Published: June 25, 2014

Research Article

Decomposition of Dynamic p-y Curves Considering Liquefaction during Earthquakes

Baydaa Hussain Maula, Tang Liang and Ali Mahommed Gazal
Foundation of Technical Education, Baghdad, Iraq

Abstract: There is an established fact known that, there is a relation between the p-y resistance of piles and liquefaction formation. To investigate this fact, a single pile foundation in liquefiable soils composed of liquefiable sand and overlying soft clay was subjected to sinusoidal shaking motions will be tested. That is the basic purpose of this study was to analyze and construct a p-y curve of liquefied soil under different shaking loading conditions companied with the effects of several key design parameters were undertaken to understand the effect of pile characteristic and pore water pressure response in the zones of responding area.

Keywords: Curve fitting, dynamic p-y, lateral resistance, liquefaction, pile stiffness ratio, sine wave

INTRODUCTION

All the accumulate damaged on the pile foundations was caused by soil liquefaction during earthquakes (Abdoun and Dobry, 2002; Boulanger *et al*., 1999). Most of that damage is a companion to the movement of the ground, which induced by this phenomenon. Trial prediction to address the p and y behavior had been done by Kagawa *et al*. (1994), Tokimatsu and Asaka (1998), Cubrinovski *et al*. (2006), Chen *et al*. (2007) and Yuan *et al*. (2010). These trial prediction was helpful by giving results which made other researchers to find the explanation of pore pressure response influences around a pile and its effect on dynamic p-y behavior, this study will be focused on p-y curves (shape, changing behavior, magnitude and developing) at various levels of pore water pressure ratio (r_u) under different shaking loading magnitude and shaping. In the next sections, simulation, protocol and results are presented.

NUMERICAL MODELING OF SHAKE-TABLE TEST SYSTEM

An open source, object-oriented nonlinear finite element analysis framework OpenSees (Mazzoni *et al*., 2009), is employed throughout the study to model geotechnical systems and simulate their response under seismic loads (http://opensees. berkeley.edu). A two-phase (fluid and solid) fully-coupled finite element formulation is adapted based on Biot (1955) theory and the saturated soil is modeled as porous media. A simplified numerical modeling of this theory, known as u-p formulation, was implemented to simulate dynamic response of soil-pile interaction in lateral spreading sand stratums and is expressed in the following matrix form (Chen *et al*., 1998):

$$\boldsymbol{M}\ddot{\boldsymbol{u}} + \boldsymbol{C}\dot{\boldsymbol{u}} + \int_{\Omega} \boldsymbol{B}^{\mathrm{T}}\boldsymbol{\sigma}' d\Omega - \boldsymbol{Q}\boldsymbol{p} = \boldsymbol{f}^{u} \tag{1}$$

$$\boldsymbol{Q}^{\mathrm{T}}\dot{\boldsymbol{u}} - \boldsymbol{S}\dot{\boldsymbol{p}} - \boldsymbol{H}\boldsymbol{p} = \boldsymbol{f}^{p} \tag{2}$$

where,
M = Total mass matrix
u = Displacement vector
B = Strain-displacement matrix
σ' = Effective stress tensor which is determined by soil constitutive model
Q = Discrete gradient operator coupling solid and fluid phases
p = Pore pressure vector
S = Compressibility matrix
H = Permeability matrix

Vectors f^u and f^p represent the effects of body forces and prescribed boundary conditions for solid-fluid mixture and fluid phase respectively.

A simplified numerical modeling of this theory, known as u-p formulation (Zienkiewicz and Shiomi, 1984; Chan, 1988), is implemented to simulate the dynamic response of saturated sand. The solid-fluid fully coupled 3D 20-8 node elements (brickUP) are used to model the saturated soil (Parra, 1996; Yang and Elgamal, 2004; Elgamal *et al*., 2002, 2003; Yang *et al*., 2003). This element is a hexahedral linear isoparametric one with dependent excess pore pressure based on the Biot's theory of porous materials, where twenty nodes represent the solid translational degrees of freedom, with the eight-corner nodes also describing the fluid pressure (Lu, 2006). The clay soil domain is expressed

Corresponding Author: Baydaa Hussain Maula, Foundation of Technical Education, Baghdad, Iraq

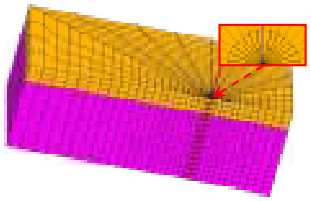

Fig. 1: Finite element modeling

by 20-node brick element without considering excess pore pressure.

Clay is modeled as a nonlinear hysteretic material (Parra, 1996; Yang and Elgamal, 2004; Yang *et al*., 2003) with a Von Mises multi-surface kinematic plasticity model (Iwan, 1967; Mroz, 1967). This model emphasizes on the reproduction of soil hysteretic Elasto-plastic shear response, including permanent deformation and the plasticity is exhibited only in the deviatoric stress-strain response (Kondner, 1963).

Model design and layouts: In the *3D* model, there is circle reinforced concrete pile-column. The pile is 0.2 m in diameter and 1.92 m in length with Young modulus equal to 2.08×10^4 (MPa) is tested to simulate the response of pile foundation subjected to soil liquefaction under nearly harmonic base excitations with dynamic sine wave. A rigid mass of 240 kg is set and fixed on the pile head as the superstructure. The soil profiles used in the test consist of two horizontal soil strata. The underlying stratum with 1.2 m thickness is modeled as saturated sand with the upper "model clay" stratum with 0.3 m thickness being weaker reconstituted silty clay. The sand stratum in each model is constructed by the sedimentation method (sand deposition in water). Water table level is located at 0.3 m near the soil interface between clay stratum and liquefiable sand stratum.

In the 3D model, the pile and column are modeled as 3D elastic beam-column elements available in FE model.

Mesh for the 3D FEM modeling is shown in Fig. 1. Length in the longitudinal direction is 3.8 m, while that in transversal direction (in this mesh configuration) is 1.5 m.

The detailed characteristics of the constitutive model for sand and clay and pile for the linear beam elements are defined in Table 1 and 2 (Al-Maula Baydaa, 2013).

Numerical modeling:

Events used in the test: The test program was listed in Table 3. The suite of shaking events began with low-level shaking and then successively progressed through very strong motions (0.5 g 1 Hz) to cause soil liquefaction.

RESULTS AND INTERPRETATION

Parametric study:

Pile characteristic effects (Pile diameter): Effect of pile diameter on soil-pile interaction at different depths is presented in Fig. 2 to 4. The lateral displacement significantly decreases with using larger diameter pile. The magnitude of lateral acceleration of pile greatly influenced by pile diameter, resulting in the decrease of y at pile head and 0.4 m depth as pile diameter increases from 0.1 m to 0.3 m (Fig. 2 to 4).

The effectiveness of pile diameter in reducing liquefaction-induce lateral displacement can further be improved by enlarging the pile diameter to provide a larger surrounding area and thus, more resistance to hold the ground deformation during an earthquake.

It could be observed that the computed soil displacements around the pile perimeter always increase gradually until they suddenly enlarge at about 3 to 5 Sec and still show higher oscillation during the shaking, which is consistent with the trend of pile bending moments on the pile. The magnitude of lateral

Table 1: Parameters for Constitutive Model of Sand (Al-Maula Baydaa, 2013)

Parameters	Medium-dense sand
Density (kg/m^3)	1900
Reference shear modulus (kPa, P_r = 80 kPa)	7.5×10^4
Reference Bulk modulus (kPa, P_r = 80 kPa)	2.0×10^5
Friction angle (degrees)	35
Peak shear strain (P_r = 80kPa)	0.1
Reference mean effective pressure (kPa)	80
Pressure dependence coefficient n_p	0.5
Phase transformation angle (degrees)	27
Contraction parameter c_1	0.08
Dilation parameter d_1	1.5
Dilation parameter d_2	2
Perfectly plastic strain parameter y_1	0.003
Perfectly plastic strain parameter y_2	1
Permeability coefficient (m/s)	9.0×10^{-6}
Possion's ratio	0.4

Table 2: Parameters for Constitutive Model of Medium Clay (Al-Maula Baydaa, 2013)

Parameters	Values
Density (kg/m^3)	1800
Reference shear modulus (kPa, P_r = 80 kPa)	6.0×10^4
Reference Bulk modulus (kPa, P_r = 80 kPa)	3.0×10^5
Cohesion (kPa)	35
Peak shear strain (P_r = 80 kPa)	0.1
Friction angle (degrees)	12
Possion's ratio	0.45
Permeability coefficient (m/s)	1.0×10^{-9}
Pressure dependence coefficients n_p	0

Table 3: Suite of shaking events

Event	Motion	Base input, A_{max} (g)
Event A	Sinsoudial earthquake	0.1g 1Hz
Event B	Sinusoidal earthquake	0.15g 2Hz
Event C	Sinusoidal earthquake	0.20 g
Event D	Sinsoudial earthquake	0.4 g
Event E	Sinusoidal earthquake	0.50 g

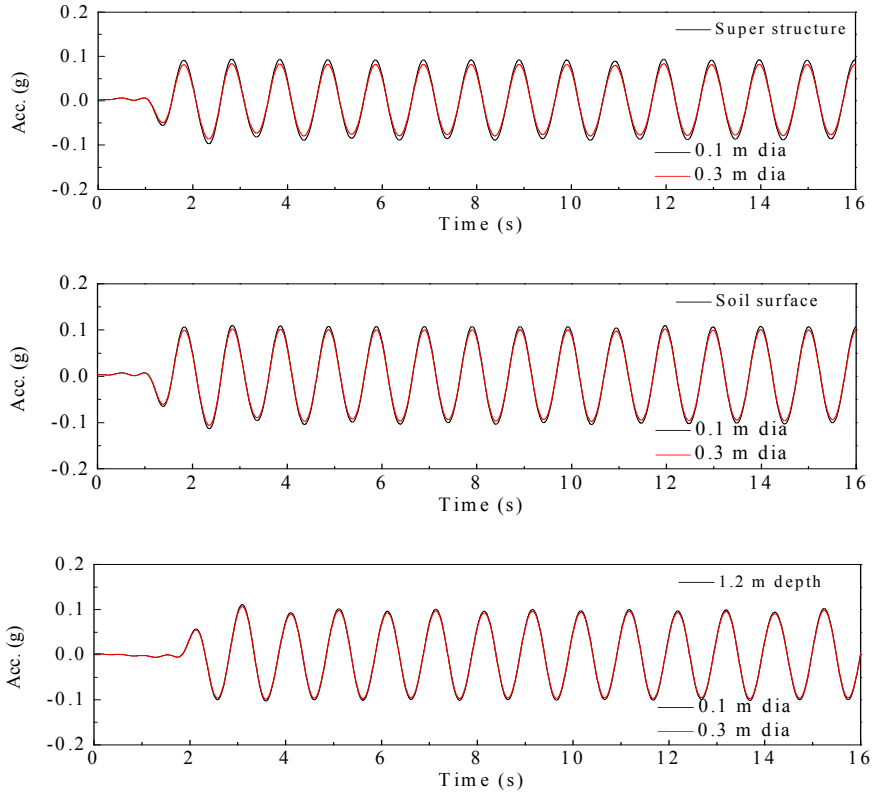

(a) Event A

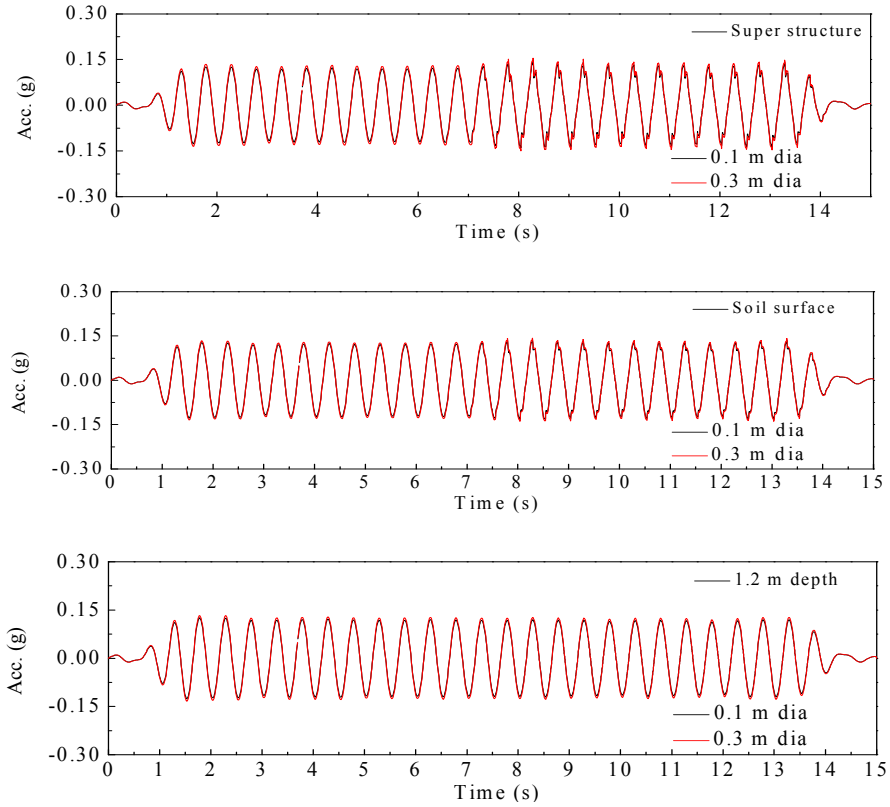

(b) Event B

Fig. 2 Comparison of acceleration time histories of pile with different diameter

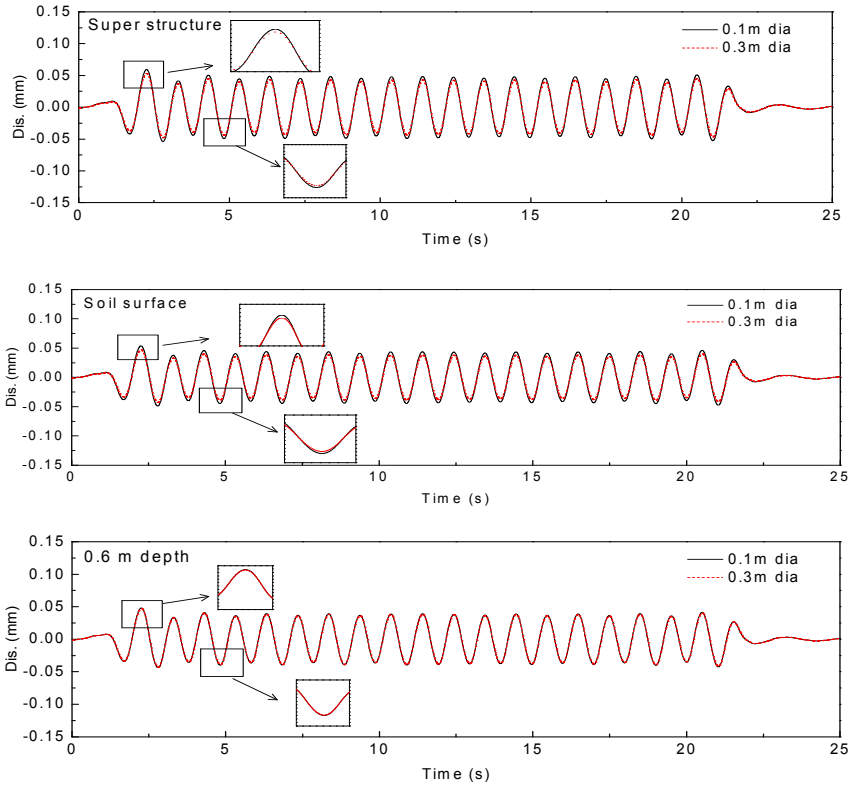

(a) Event A

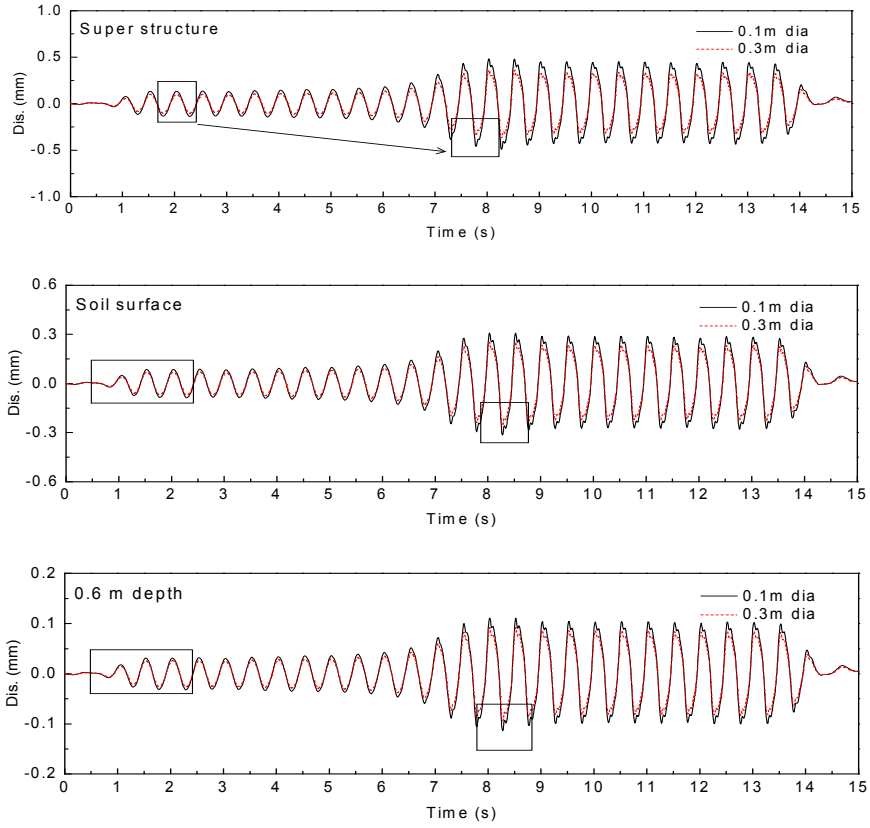

(b) Event B

Fig. 3: Displacement time histories of pile with different diameter

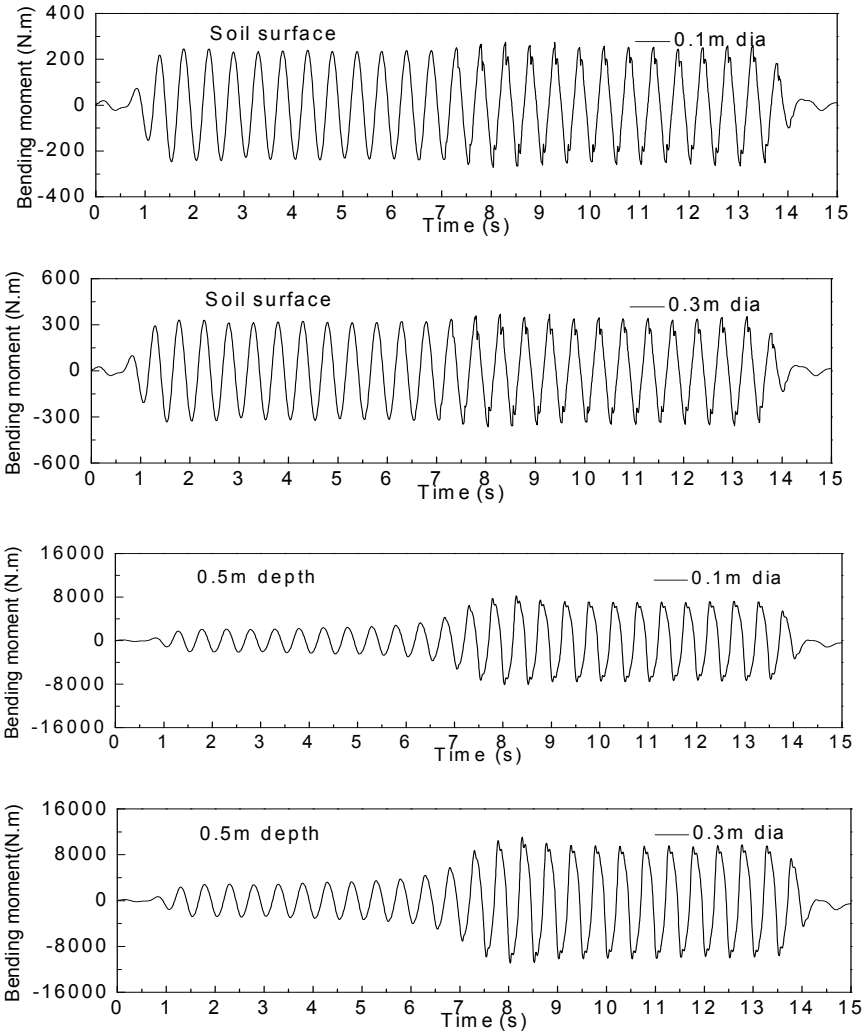

Fig. 4: Bending moment time histories of pile shaft in Event B

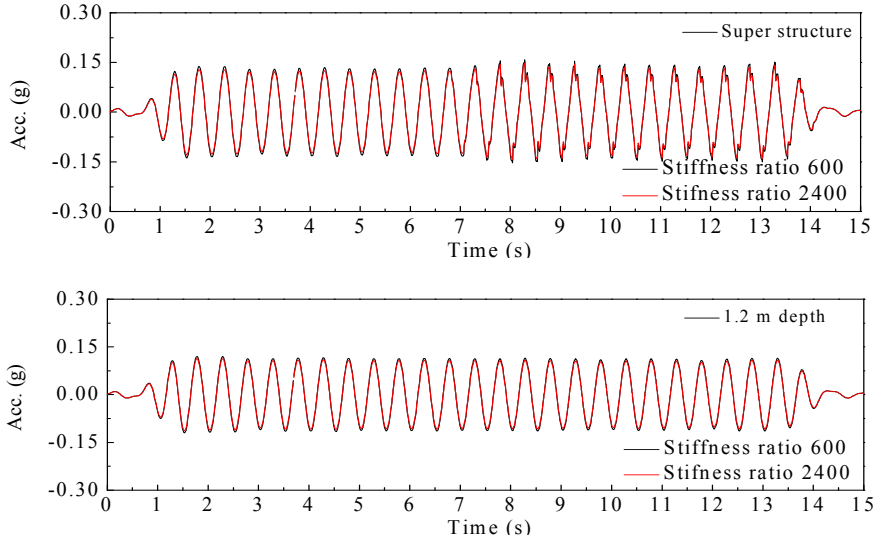

(a) Event A

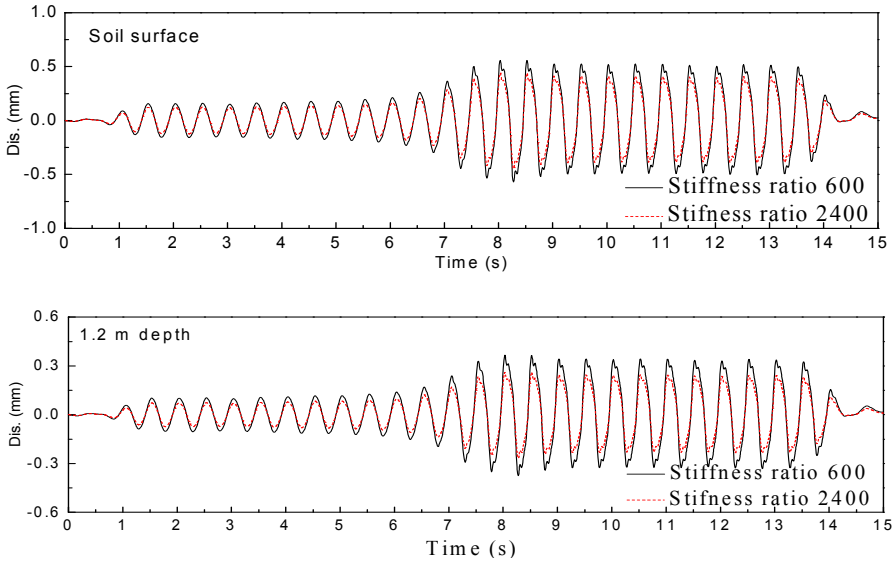

(b) Event B

Fig. 5: Comparison of acceleration time histories of pile with different stiffness ratio

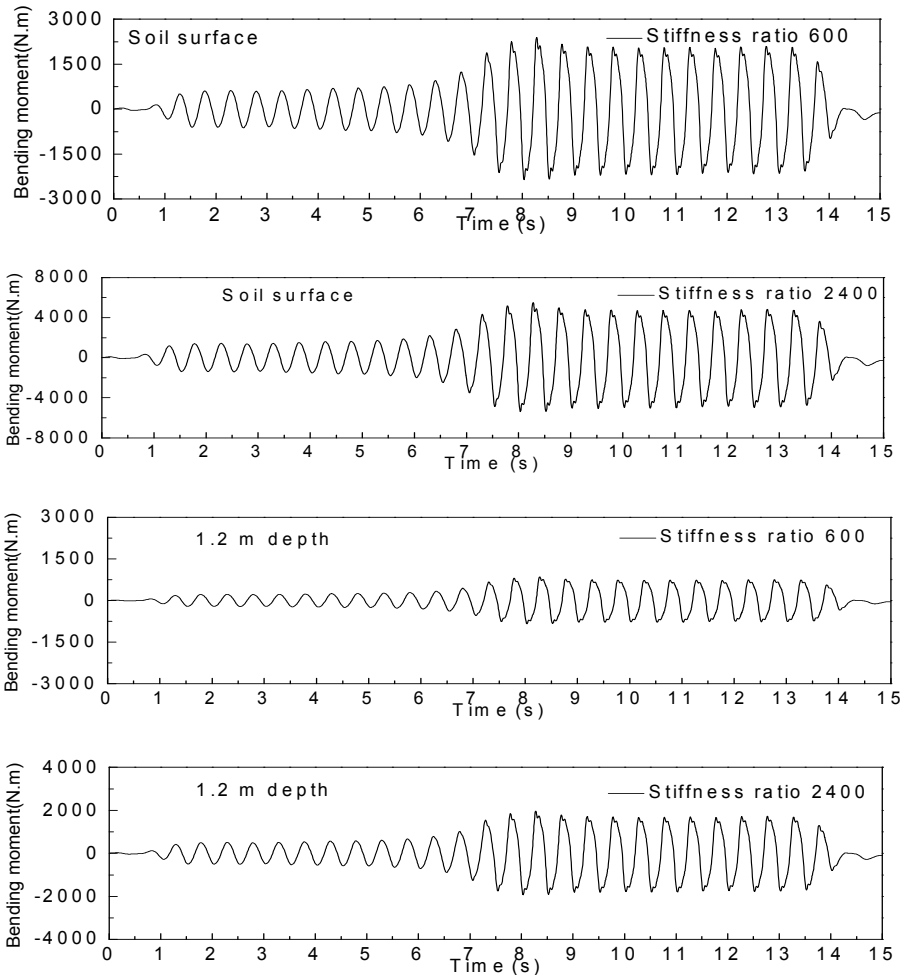

Fig. 6: Bending moment time histories of pile shaft for Event B

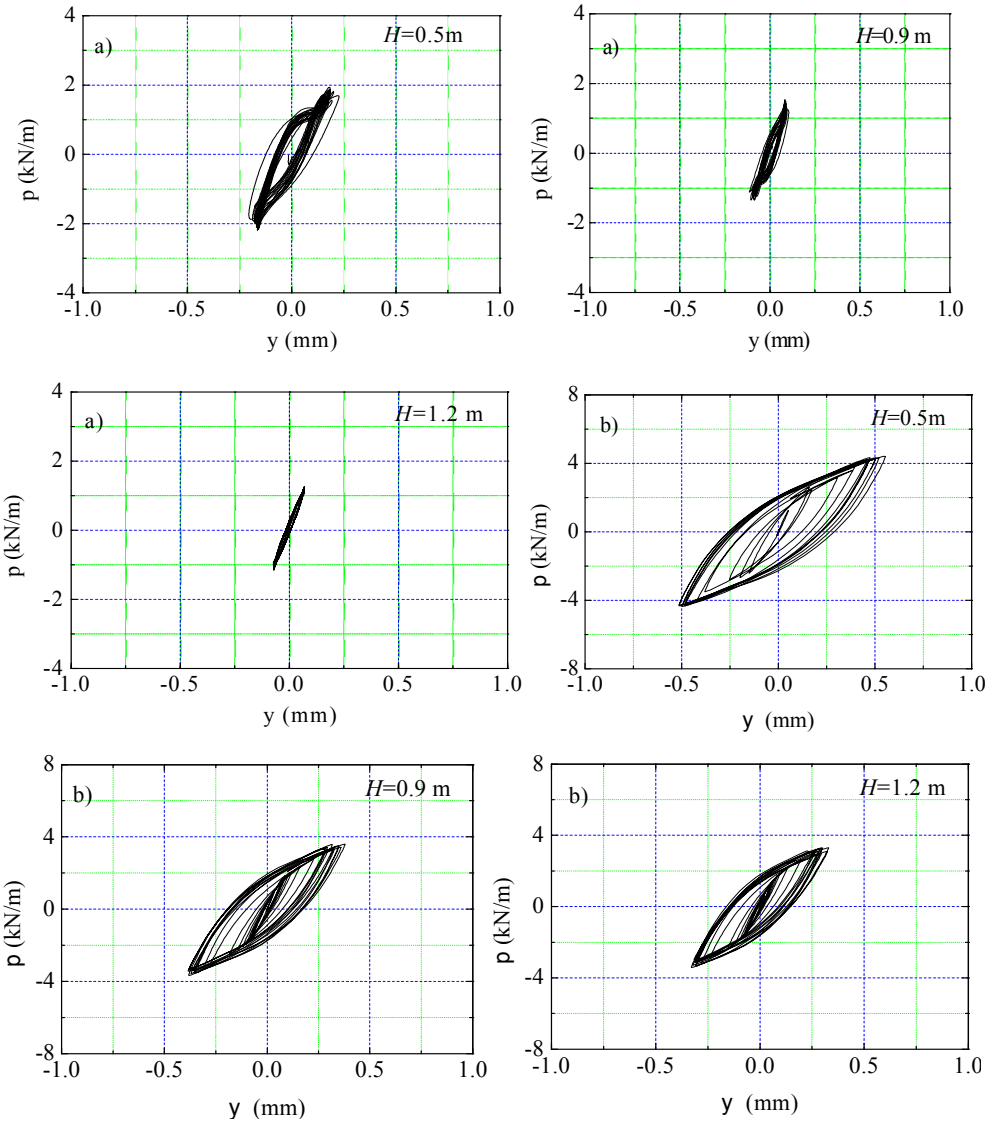

Fig. 7: Dynamic p-y curves of sand in event A and E

resistance of pile relies heavily on pile diameter, resulting in the decrease of pile bending moment at the soil surface as pile diameter increases from 0.1 m to 0.3 m Fig. 4.

Pile characteristic effects (Pile stiffness): The representative elastic moduli of pile Ep (i.e., 1.0×10^4 MPa and 4.0×10^4 MPa) are chosen where Es equal to 16.6 MPa for medium-dense sand. Figure 5 shows the effect of pile stiffness ratio as Ep/Es equal to 600 and 2400 on the lateral pile displacements. The maximum pile displacements are around 0.02 mm (Fig. 5). It is observed that the increasing pile stiffness seems to have limited effects on reducing the pile deformations (p and y). While pile acceleration time history response had anther behavior, with the stiffness ratio increases, the pile acceleration response decreases, specially at shallow depth more than at deeper depth (1.2) m, again Fig. 6 shows a smaller stiffness ratio; pile more prone to maximum bending moment.

Pore water pressure ratio Development (r_u): As mentioned earlier the basic aim of this study was to specify p-y curves at levels of r_u less than 1.0. To generate these curves, numerical simulation using OpenSeesPL will be applied to constructed these curves.

Results from the numerical p and y time histories at a depth of 0.5, 0.9 and 1.2 m are presented in Fig. 7 for event A and E earthquake event. The upper sand layer liquefied early in shaking for both events as shown in Fig. 7a and b. In event E, for early stages liquefaction take place, with produce a basic resistance (p) with larger relative displacements (y) >0.5 mm at 0.5 m

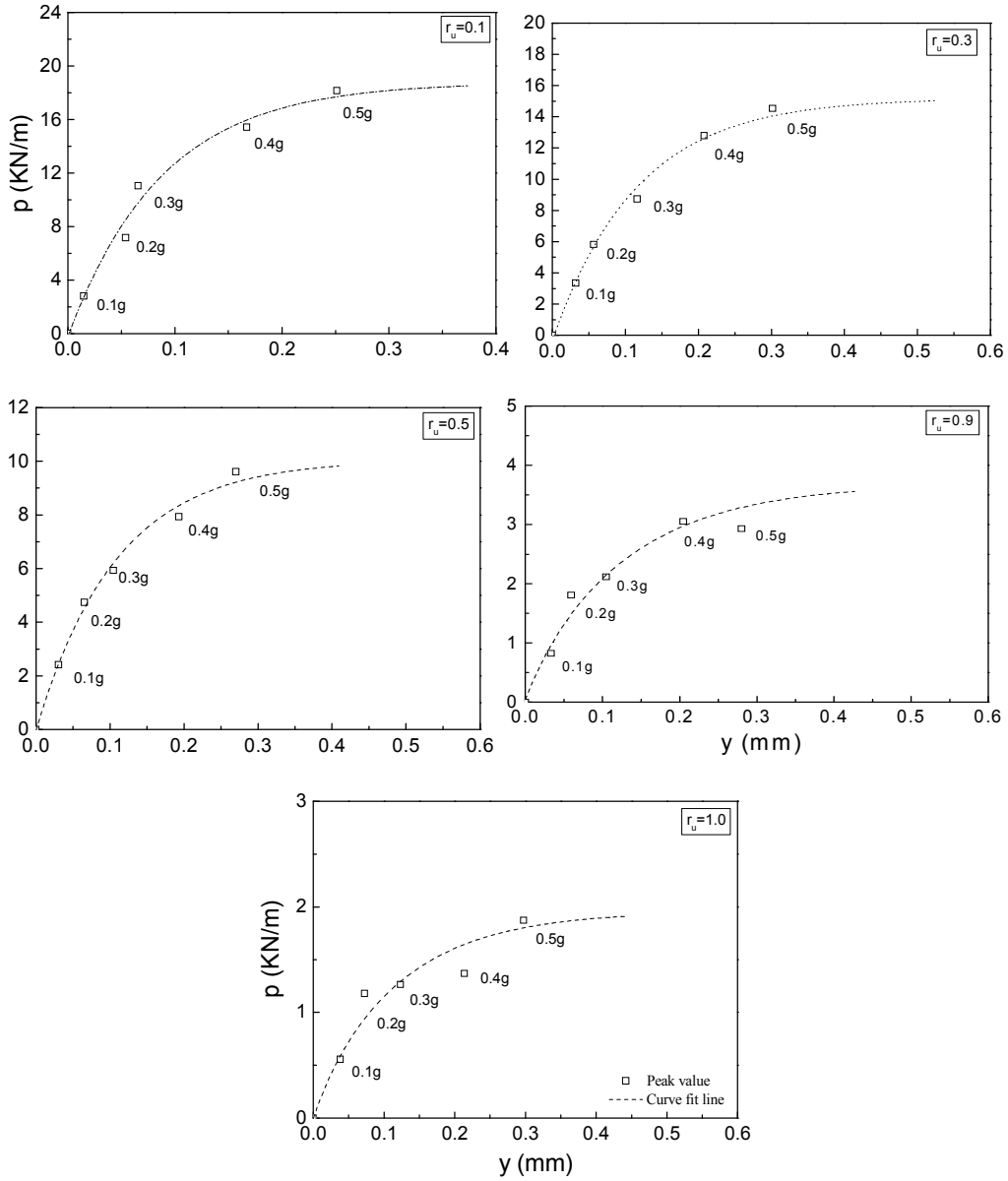

Fig. 8: Curve fitting of p-y curve for different pore pressure ratio at 0.5 m depth under Sine wave (0.1g-0.5 g 1 Hz)

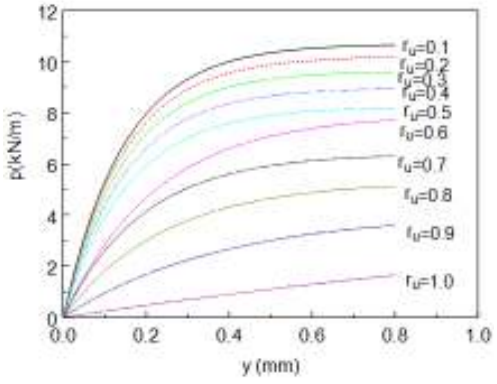

Fig. 9: Constructed p-y curve for different pore pressure ratio at 0.50 m depth under Sine wave (0.1g-0.5g 1 Hz)

depth with generated high pore pressure ratios in event E except event A, where there is no sing for liquefaction.

Figure 8 show the relationships of (y, p and r_u) as a peak value in events A to E as well as at 0.2 m pile diameter as a dynamic p-y curves as shown together in Fig. 8. The relationships of y and p and at different r_u show that the motion amplitude has a significant effect on the relative displacement at specific pore pressure ratio.

The lateral resistance (p) decreases with increasing relative displacement (y) (Fig. 8), which makes the p-y curves softening. No matter of whether the pile pushes the soil or vise versa. The increase in lateral resistance (P) has a relation with the decrease in average pore

pressure Fig. 8. The higher the lateral resistance is, during the early stage of liquefaction. This result confirm that the motion (amplitude and shaping) has a significant effect on the pore pressure reduction and the p-y behavior during liquefaction, this finding agree with the results of Fig. 8 for different earthquake amplitude.

The effect of pore pressure ratio on p-y behavior is illustrated in Fig. 9 by the curve fit for p and y (Peak value) for depth 0.5 m. The p values progressively decrease relative to y.

CONCLUSION

Numerical tests were performed using pile-supported structures founded in medium-dense (Dr ≈ 58%) sand profile and subjected to a range of earthquake input motions. Soil-pile interaction was investigated in terms of the dynamic p-y curves through under variation of r_u.

Results are presented to document the construction p-y curves under dynamic pore pressures developed using empirical curve fitting. The empirical fitting p-y curves at various levels of r_u are presented. In general, it can come to conclude that the increase in the pile diameter has an importance of substrate with little deformation of the soil during the liquefaction process, as well as an increase of soil resistance.

As summarized to the effect of pile characteristics under different cases. Note that the moment on the pile in the sand gradually increases from the bottom to the top in 600 to 2400 ratio and 0.1 to 0.3 diameters. The moment on the pile is larger in larger ratio and diameter. The time when the maximum moment occurs agrees well with the peak sand displacement in all pile characteristics effects.

REFERENCES

Abdoun, T. and R. Dobry, 2002. Evaluation of pile foundation response to lateral spreading. Soil Dyn. Earthq. Eng., 22(9-11): 1051-1058.

Al-Maula Baydaa, H., 2013. Dynamic response and simplified analysis method for bridge pile foundation in liquefiable sloping ground. Ph.D. Thesis, Harbin Institute of Technology, Harbin, China.

Biot, M., 1955. Theory of elasticity and consolidation for a porous anisotropic solid. J. Appl. Phys., 26: 182-185.

Boulanger, R.W., C.J. Curras, B.L. Kutter, D. Wilson and A. Abghari, 1999. Seismic soil-pile-structure interaction experiments and analyses. J. Geotech. Geoenviron., 125(9): 750-759.

Chan, A.H.C., 1988. A unified finite element solution to static and dynamic problems of geomechanics. Ph.D. Thesis, University of Wales, Swansea, UK.

Chen, W., F. Men and L. Jing, 1998. Shaking table test study of liquefaction of building subsoils. Earthq. Eng. Eng. Vib., 18(04): 54-60. (In Chinese)

Chen, G., H. Zhuang, X. Du, L. Li, X. Zuo and D. Zhu, 2007. Large-scale shaking table test for subway station structure built in liquefiable saturated fine sand soil. J. Earthq. Eng. Eng. Vib., 27(3): 163-170. (In Chinese)

Cubrinovski, M., T. Kokusho and K. Ishihara, 2006. Interpretation from large-scale shake-table tests on piles undergoing lateral spreading in liquefied soils. Soil Dyn. Earthq. Eng., 26(24): 275-286.

Elgamal, A., Z. Yang and E. Parra, 2002. Computational modeling of cyclic mobility and post-liquefaction site response. Soil Dyn. Earthq. Eng., 22(4): 259-271.

Elgamal, A., Z. Yang, E. Parra and A. Ragheb, 2003. Modeling of cyclic mobility in saturated cohesionless soils. Int. J. Plasticity, 19(6): 883-905.

Iwan, W.D., 1967. One a class of models for the yielding behavior of continuous and composite systems. J. Appl. Mech., 34: 612-617.

Kagawa, T., C. Minowa, H. Mizuno and A. Abe, 1994. Shaking-table tests on piles in liquefying sand. Proceedings of the 5th U.S. National Conference on Earthquake Engineering. Chicago, 4: 107-116.

Kondner, K.L., 1963. Hyperbolic stress-strain response: Cohesive soils. J. Soil Mech. Found., 89(1): 115-143.

Lu, J., 2006. Parallel finite element modeling of earthquake site response and liquefaction. Ph.D. Thesis, University of California San Diego, La Jolla, U.S.A.

Mazzoni, S., F. McKenna, M.H. Scott and G.L. Fenves, 2009. Open system for earthquake engineering simulation user manual. University of California, Berkeley.

Mroz, Z., 1967. On the description of anisotropic work hardening. J. Mech. Phys. Solids, 15: 163-175.

Parra, E., 1996. Numerical modeling of liquefaction and lateral ground deformation including cyclic mobility and dilation response in soil systems. Ph.D. Thesis, Rensselaer Polytechnic Institute, Troy, NY.

Tokimatsu, K. and Y. Asaka, 1998. Effects of liquefaction-induced ground displacements on pile performance in the 1995 hyogoken-nambu earthquake. Soils Found., 2: 163-177.

Yang, Z. and A. Elgamal, 2004. Multi-surface cyclic plasticity sand model with lode angle effect. J. Geotech. Geol. Eng., 26(3): 335-348.

Yang, Z., A. Elgamal and E. Parra, 2003. A computational model for cyclic mobility and associated shear deformation. J. Geotech. Geoenviron., 129(12): 1119-1127.

Yuan, X., Y. Li and R. Sun, 2010. Mechanism of pile foundation response in liquefiable soils under seismic cyclic ground motion. China Civil Eng. J., 41(9): 103-110.

Zienkiewicz, O.C. and T. Shiomi, 1984. Dynamic behaviour of saturated porous media: The generalized biot formulation and its numerical solution. Int. J. Numer. Meth. Eng., 8: 71-96.